

## OMAE 2008-57160

### WAVE STATISTICS AND SPECTRA VIA A VARIATIONAL WAVE ACQUISITION STEREO SYSTEM

**Guillermo Gallego**

School of Electrical & Computer Engineering  
Georgia Institute of Technology, Atlanta USA

**Alvise Benetazzo**

PROTECNO S.r.l. Padua ITALY

**Anthony Yezzi**

School of Electrical & Computer Engineering  
Georgia Institute of Technology, Atlanta USA

**Francesco Fedele**

School of Civil & Environmental Engineering  
Georgia Institute of Technology, Savannah, USA

#### ABSTRACT

We propose a novel variational Wave Acquisition Stereo System (WASS) that exploits new stereo reconstruction techniques for accurate estimates of the spatio-temporal dynamics of ocean waves. WASS has a significant advantage as a low-cost system in both installation and maintenance. A stereo camera view provides three-dimensional data (both in space and time) whose statistical content is richer than that of a time series retrieved from wave gauges, ultrasonic instruments or buoys, the latter being expensive to install and maintain. Indeed, wave spectra can be easily estimated from the multi-dimensional images obtained with WASS. The estimated spectra present an inertial range that decays as  $k^{-2.5}$ ,  $k$  being the wave number, in agreement with wave turbulence theory (Zakharov 1999, Socquet-Juglard et al. 2005). Further, the empirical probability density functions derived from the reconstructed surface data compare very well with theoretical models (Tayfun & Fedele 2007, Fedele 2008). The variational WASS is a promising technology with broader impacts in offshore engineering since it will enrich the understanding of the statistics of waves for an improved design of offshore structures.

#### STEREO VIDEO IMAGERY – AN OVERVIEW

The Wave Acquisition Stereo System (WASS) (Benetazzo 2006) utilizes stereo vision based on two calibrated views for providing time series of scattered 3-D points of the water surface (see Figures 1, 2). Water

surface topography can be measured from the conventional stereographic technique algorithms (Ma et al., 2004) used to survey geodetical surfaces or static objects. The major difference is that the water surface is a specular object in rapid movement. Thus, each stereo-pair is acquired simultaneously. First experiments with cameras mounted on an ocean going ship are by Schumacher (1939) and Cote' et al. (1960). Shemdin et al. (1988,1992) proposed the directional measurements of short ocean waves applying stereography. This experiment used a pair of cameras mounted on an oceanographic offshore tower near San Diego (USA) to create 3D model of the sea surface and then, via spectral analysis, to extract directional information of waves. The most recent integration of stereographic techniques into the field of oceanography has been the WAVESCAN project (Santel et al. 2004).

The reconstruction of the wave surface from stereo pairs of ocean wave images is a classical problem in computer vision commonly known as the correspondence problem (Klette et al., 1998, Ma et al. 2004). Its solution is based on epipolar geometry techniques that find corresponding points in the two images, from which one obtains the estimate of the real point in the three dimensional terrestrial coordinate system. WASS will process multi-dimensional image data and obtain a 4-D (space and time) reconstruction of

the sea surface. Benetazzo (2006) successfully used WASS in experiments offshore the California Coast and at the Venice coast in Italy. He was able to estimate wave spectra from the extracted time series of the surface fluctuations at one fixed point from the data images. The accuracy of such spectral estimates is as good as that from ultrasonic transducer measurements, as shown in Figure 3.



**Figure 1:** WASS physical set-up of two calibrated cameras.

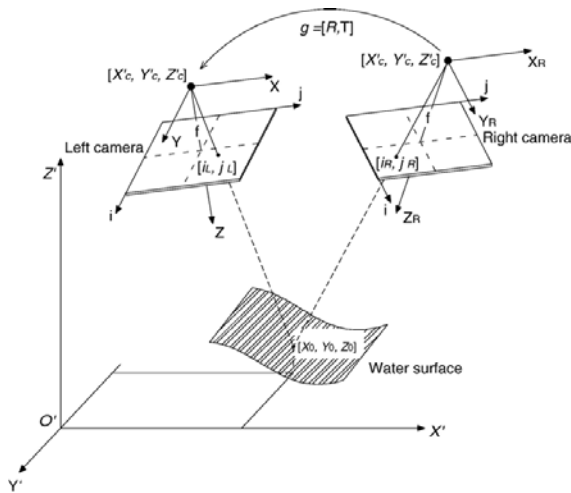


**Figure 2:** Set-up of two camera stereometric intersection (From Benetazzo, 2006). Mathematical pinhole camera model.

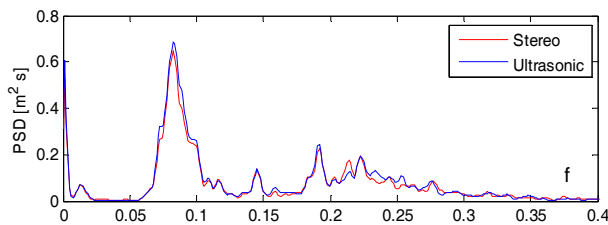


**Figure 3:** Wave spectra as function of the frequency  $f$  estimated from both stereo data and ultrasonic measurements. (From Benetazzo 2006).

## THE STEREO RECONSTRUCTION OF OCEAN WAVES

In this paper, a variational approach is considered to address the reconstruction problem in a different way from the traditional correspondence problem based on epipolar geometries. Consider the water surface supporting a Lambertian radiance function. The latter is approximately true on a cloudy day because, at a given point on the water surface, the same amount of light is received from all possible directions and reflected towards the observer causing a visual blurring of the specularities of the water. Under these conditions, the traditional stereographic algorithm based on epipolar geometries may fail to provide a smooth surface reconstruction because of “holes” corresponding to unmatched image regions (Ma et al., 2004, Benetazzo 2006).

In this paper, we address this problem by proposing a variational WASS that exploits variational partial differential equation (PDE) techniques for 3D dense and regular stereo reconstructions of the water surface. Finally, we present results showing that the variational WASS yields accurate estimates of the spatio-temporal ocean dynamics and of the associated wave spectra and statistics.

## THE VARIATIONAL GEOMETRIC METHOD

Under the assumptions of a Lambertian surface, following the seminal work by (Faugeras et al. 1998), the 3-D reconstruction of the water surface is obtained in the context of active surfaces by evolving an initial surface through a PDE derived from the gradient descent flow of a cost functional designed for the stereo reconstruction problem.

To be more specific, the energy being *maximized* is the normalized cross correlation between the image intensities obtained by projecting the same water surface patch onto both image planes of the cameras. It is clear that such energy depends on the shape of the water surface. Therefore, the active surface establishes an evolving correspondence between the pixels in both images. Hence, the correspondence will be obtained by evolving a surface in 3-D instead of just performing image-to-image intensity comparisons without an explicit 3-D model of the target surface being reconstructed.

## Notation

Consider the same set-up of the WASS, in which two calibrated cameras are viewing the water surface. Quantities corresponding to the left (resp. right) camera will be noted with a “1” (resp. “2”) subscript. If the projection matrices that model the perspective projection of the cameras are known with respect to the left camera coordinate system, then  $P_1 = K_1(I,0)$  and  $P_2 = K_2(R,t)$ , where  $K_1, K_2$  are the intrinsic parameter matrices (containing the focal lengths, principal points and skews) and  $g = (R,t)$  defines the rigid transformation between both camera coordinate systems. Let  $X = (x, y, z)^t$  represent a generic 3-D point in the scene, expressed with respect to the same coordinate system as the projection matrices. As it is well known, the equations that model the geometry of the image formation process are linear in homogeneous coordinates form: a 3-D point  $\bar{X} = (x, y, z, 1)^t$  maps to the image points  $\bar{x}_i = (u_i, v_i, 1)^t \sim P_i \bar{X}$ , ( $i=1,2$ ), where  $\sim$  means equality up to a non-zero scale factor. Therefore,  $x_i = (u_i, v_i)^t$  are the pixel coordinates of the image points. Let  $\pi_i : R^3 \rightarrow R^2$  note the perspective projection maps:  $x_i = \pi_i(X)$ , ( $i=1,2$ ).

The primary object of interest will be a regular surface  $S$  in  $R^3$  (with area element  $dA$ ), representing the water surface. As it will be shown later in the implementation of the algorithm, the surface  $S$  will be represented as the zero level set of a smooth function  $\hat{U} : R^3 \rightarrow R$ , i.e.,  $S = \{X | \hat{U}(X) = 0\}$ .

### Cost functional

To infer the shape of the water surface  $S$ , we set up a cost functional on the discrepancy between the projection of the model surface and the image measurements. As previously announced, such cost is based on a cross correlation measure between image intensities, which will be noted as  $E_{data}(S)$ . We conjecture that, to have a well-posed problem, a regularization term that imposes a geometric prior must also be included,  $E_{geom}(S)$ . We consider the cost functional to be the (weighted) sum:

$$E(S) = E_{data}(S) + E_{geom}(S). \quad (1)$$

In particular, the geometric term favours surfaces of least area:

$$E_{geom}(S) = \int_S dA. \quad (2)$$

The data fidelity term may be expressed as

$$E_{data}(S) = \int_S \left( 1 - \frac{\langle I_1, I_2 \rangle}{|I_1| |I_2|} \right) dA, \quad (3)$$

where only the surface in a region within the field of views of both cameras is considered. The unnormalized cross-correlation between  $I_1$  and  $I_2$  corresponding to a common 3-D point  $X$  that projects on the pixels  $x_1 = \pi_1(X)$ ,  $x_2 = \pi_2(X)$ , is

$$\langle I_1, I_2 \rangle(S) = \frac{1}{4pq} \int_{-p}^p \int_{-q}^q [I_1(\pi_1(X+m)) - \bar{I}_1(x_1)] [I_2(\pi_2(X+m)) - \bar{I}_2(x_2)] dm$$

where the integration is over a small patch in the tangent plane  $T_S$  to the water surface  $S$  at  $X$  and, therefore, the averages  $\bar{I}_i(x_i)$  are defined as

$$\bar{I}_i(x_i) = \frac{1}{4pq} \int_{-p}^p \int_{-q}^q I_i(\pi_i(X+m')) dm', \quad (i=1,2).$$

We note  $|I|^2 = \langle I, I \rangle$ . Observe that this definition of  $\langle I_1, I_2 \rangle$  is symmetric and, therefore, the term  $\langle I_2, I_1 \rangle$  is already included in  $E_{data}(S)$ . The term  $+1$  in (3) yields a positive energy, which prevents antidiffusive terms from occurring in the following evolution equation.

### Evolution equation

To find the surface  $S$  that minimizes  $E(S)$ , we start from an initial estimate of the surface at time  $t = 0$ ,  $S_0$ , and set up a gradient flow based on the first variation of  $E(S)$  that will make the surface evolve towards a minimizer of  $E(S)$ , hopefully converging to the desired water surface shape.

Based on the theorem in (Faugeras et al. 1998) that says that for a function  $\Phi : R^3 \rightarrow R^+$  and the energy

$$E = \int_S \Phi(X, N) dA, \quad (4)$$

where  $N$  is the unit normal to  $S$  at  $X$ , the flow that minimizes  $E$  is given by the evolution PDE

$$S_t = \beta N, \quad (5)$$

where  $S_t$  is the derivative of  $S$  with respect to time and the speed function  $\beta$  is

$$\beta = 2H(\Phi - \Phi_{N \cdot N}) - \Phi_X \cdot N - \text{trace} \left[ (\Phi_{XN})_{T_S} + dN \circ (\Phi_{NN})_{T_S} \right]$$

All quantities are evaluated at the point  $S=X$  with normal  $N$  to the surface.  $H$  denotes the mean curvature.  $\Phi_X, \Phi_N$  are the first-order derivatives of  $\Phi$ , while  $\Phi_{XN}, \Phi_{NN}$  are

the second-order derivatives.  $dN$  is the differential of the Gauss map of the surface and  $(\cdot)_{T_S}$  means “restriction to the tangent plane  $T_S$  to the surface at  $S=X$ ”.

Note that our proposed energy (1) can be expressed in the form of (4) if

$$\Phi = \left( 1 - \frac{\langle I_1, I_2 \rangle}{|I_1| |I_2|} \right) + \alpha,$$

where  $\alpha$  is just a weight for the geometric prior. In practice, we use the flow based on the first-order derivatives of  $\Phi$  because it provides similar results to those of the complete expression, but saves a significant amount of computations,

$$S_t = (2H(\Phi - \Phi_N \cdot N) - \Phi_X \cdot N)N. \quad (6)$$

The level set framework (Osher et al. 1988) has been adopted to numerically implement (6). This formulation requires an implicit representation of the surface. At each time  $t$ , the surface  $S$  is the zero level set of the level set function  $U: \mathbb{R}^4 \rightarrow \mathbb{R}$ , i.e.,

$$S \text{ at time } t \text{ is } \{X \in \mathbb{R}^3 \mid U(X, t) = 0\}.$$

The unit normal of the surface is  $N = -\nabla U / |\nabla U|$ , where  $\nabla$  stands for the derivatives with respect to the first three coordinates of  $U$ . The evolution equation for the level set function  $U$  corresponding to the evolution equation for the surface (5) is

$$U_t = \beta |\nabla U|. \quad (7)$$

In a numerical implementation, the level set function  $U$  is discretized in a 3-D grid enclosing the volume of interest in the world where the water surface is known to be. The derivatives of  $\Phi$ , the mean curvature  $H$ , the unit normal vector  $N$ , etc. are approximated by numerical finite difference formulas. After the evolution, the surface itself is extracted using the marching cube algorithm, which is a very popular routine, such as MATLAB’s isosurface command.

### Initialization

As is well known, a good initialization is strongly encouraged in gradient descent algorithms to mitigate the problem of getting stuck in a local minimum far away from the desired solution. A sensible initialization for the proposed variational stereo algorithm is to consider the surface at time  $t=0$  to be the simplest (lowest frequency) approximation to the water surface, i.e., a plane (flat surface).

In the experiments, this approximation is computed from a set of 10 to 15 manually matched point correspondences  $\{x_1^k \leftrightarrow x_2^k\}_{k=1}^n$  between both images. Since the cameras are calibrated, a triangulation (back-

projection) algorithm may be used to find the approximate location of the 3-D points  $\{X_k\}_{k=1}^n$  that project onto  $x_1^k, x_2^k$  because  $X_k = f(P_1, P_2, x_1^k, x_2^k)$ . Then, a plane can be fitted to this set of 3-D points by minimizing a least-square criterion such as the orthogonal distance to the points. Once this plane is known, the level set function  $U(X,0)$  is initialized as the signed distance function to the plane and the algorithm can be run to evolve the surface.

Observe that if the plane is known, one may also back-project the four corners of each image and intersect those optical rays with the plane to obtain an estimate of the quadrilateral field of view of the cameras on the plane. This is also used to set up the volume where the level set function is discretized.

### Camera to terrestrial coordinates

Now, suppose that the variational stereo algorithm has converged. Next, the surface must be extracted from the level set and prepared for post-processing (statistical analysis, etc.). So far, the coordinate system used has been that of the (left) camera, but under the assumption that the water surface can be expressed in the form of a graph  $z' = f(x', y')$  in some terrestrial coordinate system (prime notation) related to the former by a rigid transformation, we would like to obtain such a representation of the reconstructed surface so that relevant information contained in the heights of the points on the surface may be analyzed.

The problem now can be posed as the joint estimation of the “average” plane through the surface and the rigid transformation  $(R, T)$  that moves the former to its canonical location  $z' = 0$ . We follow a decoupling strategy: first, the best plane through the data is estimated; second this plane is reoriented by a rigid transformation to become the plane  $z' = 0$ .

We now present a method that estimates the mean plane through a set of 3-D points by minimizing the geometric orthogonal distance from the points to the plane. This is a sensible criterion and provides a plane that has zero mean signed distance to the given data points.

The signed perpendicular distance from a 3-D point  $\bar{X} = (x, y, z, 1)^t$  to a plane whose coefficients (or homogeneous coordinates) are  $v = (a, b, c, d)^t$  is

$$sd(X, v) = \frac{\bar{X}^t v}{\sqrt{a^2 + b^2 + c^2}} = \frac{ax + by + cz + d}{\sqrt{a^2 + b^2 + c^2}} \quad (8)$$

and the perpendicular distance is its absolute value,

$$d(X, v) = |sd(X, v)|. \quad (9)$$

Given  $m$  points, the plane that minimizes

$$\sum_{i=1}^m d^2(X_i, v) \quad (10)$$

is defined up to a scaling of the coefficients. This degree of freedom disappears after enforcing  $|n|^2 = a^2 + b^2 + c^2 = 1$  on the magnitude of the normal to the plane,  $n = (a, b, c)^t$ . It can be shown that the minimizer of (10) satisfies a generalized eigenvalue equation. However, the following simpler procedure gives the same results.

Given  $m^3$  points  $X_i = (x_i, y_i, z_i)^t$ ,

1) *Normalization*. Apply a similarity transformation  $H_S$  (rotation, translation and isotropic scaling) to the points such that the new centroid of the points is placed at the origin and the average distance of the transformed points to the origin is  $\sqrt{3}$ .

2) *Estimation*. Compute the Singular Value Decomposition of the  $m^3$  matrix  $A$  whose  $i$ -th row is  $(x_i, y_i, z_i)$ , i.e.,  $A = UDV^t$ . Set  $\tilde{v} = (a, b, c, 0)^t$ , where  $\tilde{n} = (a, b, c)^t$  is the unit right singular vector of  $A$  associated to its smallest singular value.

3) *Denormalization*. Set  $v = H_S^t \tilde{v}$ , where  $H_S$  is the  $4 \times 4$  matrix of the similarity transformation (in homogeneous coordinates).

It can be shown that the plane estimated this way minimizes (10) and is one of the mean planes with respect to signed distance, i.e., satisfies

$$\sum_{i=1}^m sd(X_i, v) = 0. \quad (11)$$

Once the plane  $v$  is known, the goal is to find the Euclidean transformation  $(R, T)$  that moves the plane  $v$  to its canonical location in the terrestrial coordinate system.

Let  $v = (n^t, d)^t$ , if points  $\bar{X}$  transform as

$$\bar{X}' = H_E \bar{X}, \text{ where } H_E = \begin{bmatrix} R & T \\ 0^t & 1 \end{bmatrix} \quad (12)$$

is the  $4 \times 4$  matrix of the Euclidean transformation between coordinate systems, then planes transform as  $v' = H_E^{-t} v$ . The goal is to find  $R$  and  $T$  such that  $v' = (n'^t, d')^t = (0, 0, 1, 0)^t$ . This yields two equations:  $n' = (0, 0, 1)^t = Rn$  and  $T^t Rn = d$ . Observe that  $R$  is the mapping between normal vectors. The angle and axis of rotation are given by the magnitude and direction of the

cross product  $w = n \times n'$ . Rodrigues' rotation formula can be used to compute  $R$ :

$$R = I + \sin \theta [\hat{w}]_{\times} + (1 - \cos \theta) [\hat{w}]_{\times}^2, \quad (13)$$

where  $\hat{w} = w / |w|$  and  $[a]_{\times}$  is the antisymmetric matrix such that  $[a]_{\times} b = a \times b$ . If  $|n| = 1$ , then the expression for  $R$  in (13) simplifies to

$$R = \begin{bmatrix} 1 - a^2 q & -abq & -a \\ -abq & 1 - b^2 q & -b \\ a & b & c \end{bmatrix},$$

where

$$q = \frac{1 - c}{a^2 + b^2}.$$

The second equation,  $T^t Rn = d$ , has an infinite number of solutions since only the third coordinate of  $T$  is relevant. The first two coordinates of  $T$  may be used to specify the origin of terrestrial coordinates on the plane  $z' = 0$ . We may choose  $T = (0, 0, d)^t$ .

Finally, convert the water surface points from the camera coordinate system to the terrestrial coordinate system by  $X' = RX + T$ .

The reconstruction process described above is repeated for each pair of images acquired by the calibrated cameras. So far, no dynamics of the physics of the waves have been included in the model to make a joint spatio-temporal reconstruction of the water surface. This approach is postponed for future research.

## EXPERIMENTS

The data used to test the variational reconstruction algorithm is a set of images acquired by the WASS developed by Benetazzo (2006a,b); in particular, the San Diego experiment described therein. The images of waves, on water depth of 8 meters, were cropped to  $504 \times 336$  pixels to decrease the depth of the field of view of the cameras, i.e., to focus in the region close to the cameras. The baseline between the cameras is 3.04 meters and the reconstructed surface occupies a rectangle of approximately  $8 \times 8.7$  m<sup>2</sup>.

Figure 4 shows the domain of the reconstructed surface on each pair of input images to the algorithm. The level set function was discretized on a 3-D grid of  $256^3$  points and evolved during 100 iterations for every pair of images, with a time step of 0.25.

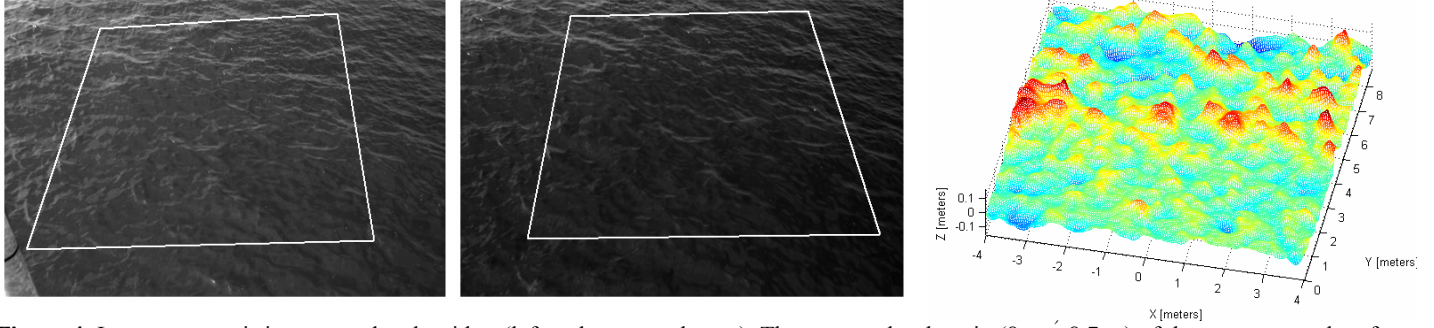


**Figure 4:** Input stereo pair images to the algorithm (left and center columns). The rectangular domain (8 m × 8.7 m) of the reconstructed surface or elevation map (right column) has been superimposed. The height of the waves is in the range  $\pm 0.2$  cm.

The distance between adjacent grid points is 8.2 cm, which is related to the maximum quantization error. The distance between adjacent grid points is 8.2 cm, which is related to the maximum quantization error. The surface is then extracted and reoriented for post-processing, as explained in the previous section. The reconstructed surface, as elevation maps is also displayed in Figure 4 (right column). The variational algorithm runs on a Intel® Core™ single Processor (2.60GHz) and the CPU time spent for the surface reconstruction is of the order of 0.5-1 minutes. On-going research effort is put in to developing faster algorithms that run on multi-core parallel machines.

## WAVE SPECTRA & STATISTICS

Herein, we elaborate the nature of the reconstructed wave surface shown in Figure 4. We point out that the following statistical analysis only exploits data from the reconstructed spatial snapshot of the ocean surface at a fixed instant of the time. We show that information content of a single spatial snapshot of the ocean surface is richer than that of traditional time series measurements. Indeed, we compute estimates of the wave spectra and provide evidences that recent probabilistic wave models (Tayfun & Fedele 2007, Fedele 2008) well explain realistic oceanic conditions.

In particular, the wave spectrum  $S(k)$  as function of the wave number  $k$  is given in Figure 5. Its tail shows an inertial range that decays as  $k^{-2.5}$  in agreement with wave turbulence theory (Zakharov 1999, Janssen 2003, Socquet-Juglard et al. 2005). Deviations of large surface heights from the Gaussian conditions are expected since water waves present steep crests and shallow troughs (Longuet-Higgins 1963, Tayfun 1980;1986, Tayfun & Fedele 2007, Fedele 2008). This is also confirmed by our analysis. Indeed, Figure 6 shows that the empirical probability density function  $p_\eta$  derived from the

reconstructed surface  $\eta$  compare very well with the Gram-Charlier models (Longuet-Higgins 1963, Tayfun & Fedele, 2007) given by

$$p_\eta(x) = \frac{\exp(-x^2/2)}{\sqrt{2\pi}} \left[ 1 + \frac{\lambda_3}{6} x(x^2 - 3) + \frac{\lambda_3^2}{72} (x^6 - 15x^4 + 45x^2 - 15) + \frac{\lambda_4}{24} (x^4 - 6x^2 + 3) \right], \quad (13)$$

where  $\lambda_3$  and  $\lambda_4$  are the skewness and kurtosis of the wave surface, respectively. These parameters characterize the nonlinear features of ocean waves and can be estimated from the video data as follows.

Drawing on Tayfun (1994), we first evaluate the probability of positive wave elevations given by

$$P^+ = \Pr\{\eta > 0\} = \frac{1}{2} - \frac{\lambda_3}{6\sqrt{2\pi}}, \quad (14)$$

where we have used

$$\Pr\{\eta > z\} = \int_z^\infty p_\eta dx = \frac{1}{2} \operatorname{erfc}\left(\frac{z}{\sqrt{2}}\right) + \frac{1}{2\sqrt{2\pi}} \exp\left(-\frac{z^2}{2}\right) \cdot \left( \frac{\lambda_3}{3} (z^2 - 1) + \frac{\lambda_4}{12} z(z^2 - 3) + \frac{\lambda_3^2}{36} z(z^4 - 10z^2 + 15) \right). \quad (15)$$

Note that  $P^+ < 1/2$  reflecting the asymmetry of wave crest and troughs. Estimates for  $\lambda_3$  follow from (14) as

$$\lambda_3 = 3\sqrt{2\pi}(1 - 2P^+), \quad (16)$$

where  $P^+$  is estimated from the surface data. The kurtosis  $\lambda_4$  could be estimated from the average positive wave height  $\overline{|\eta| \mid \eta > 0}$ , but this leads to overestimation. We thus simply estimate  $\lambda_4$  from data.

Further, in Figure 7 it is plotted the conditional probability  $p(\eta > z \mid \eta > 0)$  which agrees with the Gram-Charlier model (Longuet-Higgins 1963).

We thus have scientific evidences that the variational WASS provides accurate estimates of the spatio-temporal ocean dynamics.

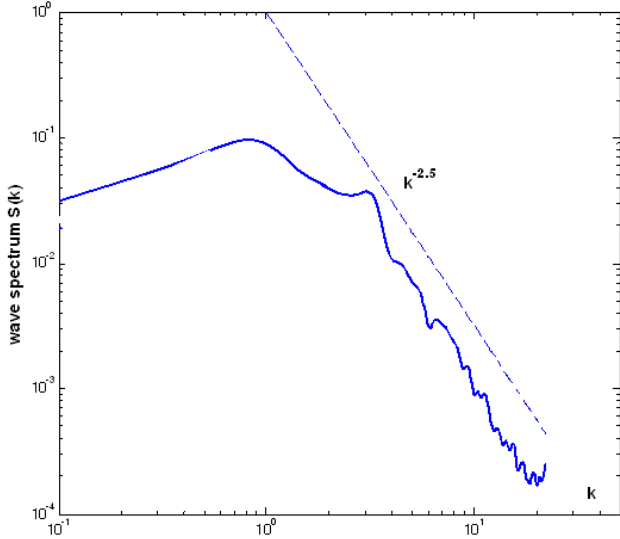


**Figure 5.** Wave spectrum  $S(k)$  as function of the wave number  $k$  computed from the reconstructed wave surface  $\eta$  in Figure 4. The spectrum tail decays as  $k^{-2.5}$  in agreement with wave turbulence theory (Zakharov 1999, Socquet-Juglard et al. 2005).

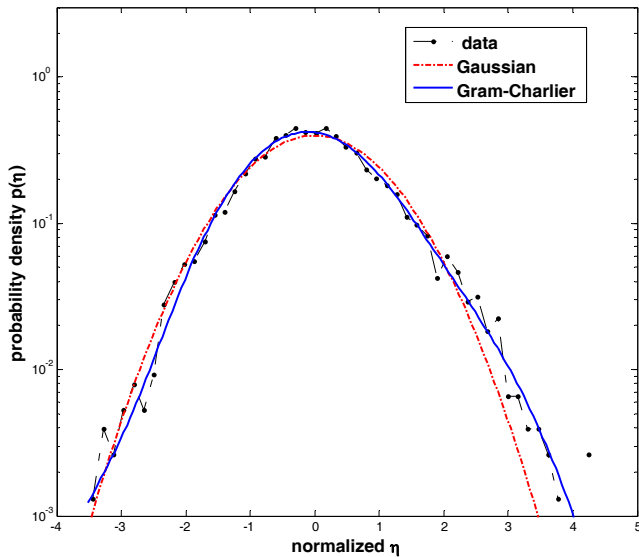


**Figure 6.** Probability density  $p(\eta)$  of the reconstructed wave surface  $\eta$  in Figure 4: comparisons with the Gram-Charlier model (Longuet-Higgins 1963, Tayfun & Fedele 2007, Fedele 2008).

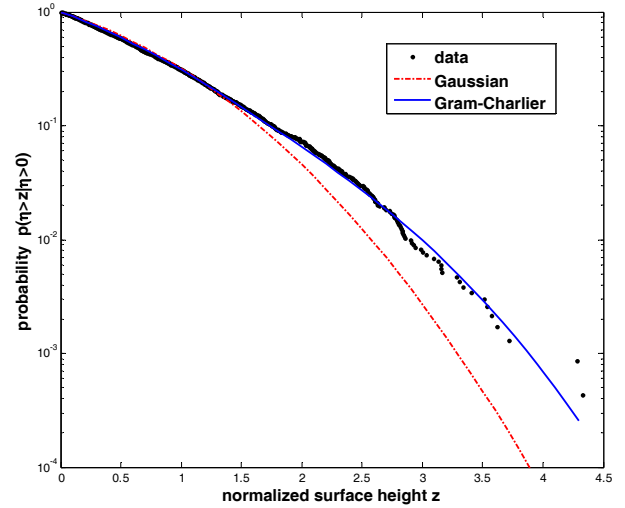


**Figure 7.** Conditional probability density  $p(\eta > z | \eta > 0)$  of the reconstructed wave surface  $\eta$  in Figure 4: comparisons with the Gram-Charlier model (Longuet-Higgins 1963, Fedele & Tayfun 2007, Fedele 2008).

## DISCUSSION AND FUTURE WORK

In this paper we have explored the possibilities of applying a variational algorithm for the stereo reconstruction of ocean waves. In particular, we have proposed a variational WASS which has the following main advantages: i) it provides a dense reconstruction of the water surface (there are no “holes” corresponding to unmatched image regions); ii) it has built in regularity due to the mean curvature component of the flow (6); iii) it yields reliable statistics of ocean waves due to the rich information content of video data.

However, this method is sensitive to specular reflections and time consuming (non real-time). These issues are subject of future work that aims improving the reconstruction algorithm by considering the dynamics of the waves and the estimation of the surface radiance function (Yezzi et al. 2001). These may be included in the cost functional and will ultimately provide a robust generative model of the images.

Further, the proposed variational geometric algorithm is very general and allows for the reconstruction of complicated surfaces. It has not been particularized yet for the case of water surface, which admits a simplified representation in the form of a graph, i.e., a point on the surface may be represented as  $X = (x, y, z(x, y))^t$ . This is a topic of future research.

We thus strongly believe that the variational WASS technology and its generalization are beneficial to

offshore industries. More accurate predictions of wave spectra and large waves in sea storms around offshore structures can be provided. In particular, reliable estimates of the highest wave expected over an area (Forristall 2005) can be computed by processing wave surface data extracted from video-imagery. Further, video data will also support the validation of theoretical models for crest or wave height exceedances (Tayfun 1986,2006, Fedele 2006, Tayfun & Fedele 2007). We point out that the highest expected wave over an area is naturally higher than the expected wave height at one point (Forristall 2005). This reflects the common sense of the surfers that wander around a site, and always find their big waves. Thus, the probability to encounter a big wave within an area of the ocean increases with its size. The proposed variational WASS will allow a better understanding of the statistics of large waves over an area, and it may yield new insights for an improved design of platforms that avoid the localized damages sometime observed on their lower decks after storms.

#### ACKNOWLEDGMENTS

The authors would like to acknowledge Hailin Jin for providing source code that was partly used to obtain the results shown in this paper. Alvise Benetazzo is also grateful to Professor Ken Melville and Luc Lenain, of the Scripps Institution of Oceanography (SIO), San Diego, for the support received. We also thank both M. Aziz Tayfun & Harald Krogstad for useful discussions and suggestions.

#### REFERENCES

Benetazzo, A. 2006a. Measurements of short water waves using stereo matched image sequences Coastal Engineering, 53:1013-1032

Benetazzo, A., 2006b. Measurement of water surface wave fields using a non-intrusive method based on a stereo-matching algorithm. Ph.D. Diss., University of Padua.

Cote', LJ, Davis, JO, Marks, W., McGough, RJ, Mehr, E., Pierson, WJ, Ropek, JF, Stephenson, G., Vetter, RC 1960. The directional spectrum of wind generated sea as determined from data obtained by the stereo wave observation project. *Meteorological paper*, 2(6), New York University, College of Engineering.

Faugeras O. & Keriven R. Variational principles, surface evolution, pde's, level set methods and the stereo problem. *IEEE Trans. on Image Processing*, 7(3):336-344, 1998.

Fedele, F. 2006. Extreme events in nonlinear random seas. *ASME Journal Offshore Mechanics and Arctic Engineering* 128(1), 11-16.

Fedele, F. 2008. Rogue Waves in Oceanic Turbulence. *Physica D* (to appear).

Forristall, GZ 2005. Understanding rogue waves: Are new physics really necessary? 14th Aha Huliko'a Hawaiian Winter Workshop, University of Hawaii

Janssen, P.A.E.M. 2003. Nonlinear four-wave interactions and freak waves. *J. Phys. Oceanogr.* 33(4):863-884.

Klette, R., Schluns, K, Koschan A. 1998. *Three-dimensional data from images*. Springer, Singapore

Krogstad H. 1988 Maximum Likelihood Estimation of Ocean Wave Spectra from General Arrays of Wave Gauges. *Modeling, Identification, and Control*, 9(2):81-97.

Longuet-Higgins, M.S. 1963. The effects of non-linearities on statistical distributions in the theory of sea waves. *J. Fluid Mech.* 17,459-480.

Ma, Y. Soatto, S., Kosecka, J., Shankar Sastry, S., 2004. *An invitation to 3-D vision: from images to geometric models*. Springer-Verlag New York

Osher S. & Sethian J. 1988 Fronts propagating with curvature-dependent speed: algorithms based on Hamilton-Jacobi equations. *J. of Comp. Physics*, 79:12-49.

Socquet-Juglard, H., Dysthe, K., Trulsen, K., Krogstad, H. E. & Liu, J. 2005. Probability distributions of surface gravity waves during spectral changes. *Journal of Fluid Mechanics* 542:195-216.

Santel F., Linder W., Heipke C. 2004 Stereoscopic 3D-Image Sequence Analysis of Sea Surfaces. *Proceedings of the ISPRS Commission V Symposium*, vol. XXXV, part 5: pp. 708-712.

Schumacher, A. 1939. Stereophotogrammetrische Wellenaufnahmen. *Wiss. Ergeb. Dtsch. Atlant. Exped. Forschungs Vermessung. 'Meteor' 1925-1927, Ozeanographische Sonderuntersuchungen, Erste Lieferung*, Berlin.

Shemdin, OH, Tran HM, Wu SC 1988. Directional measurements of short ocean waves with stereography. *J. Geophys. Res.*, 93:13891-13901

Shemdin, OH, Tran, HM, 1992. Measuring Short Surface Waves with Stereography. *Photogrammetric Engineering & Remote Sensing*, 58:311-316.

Shankar Sastry, S., 2004. *An invitation to 3-D vision: from images to geometric models*. Springer-Verlag New York

Tayfun, MA 1986. On narrow-band representation of ocean waves. Part I: Theory. *J. Geophys. Res.*, (1(C6):7743-7752

Tayfun, MA 1994. Distributions of envelope and phase in weakly nonlinear random waves. *ASCE Journal of Engineering Mechanics*, 120(4):1009-1025

Tayfun, MA 2006. Statistics of nonlinear wave crests and groups. *Ocean Engineering*, 33(11-12): 1589-1622

Tayfun, A., Fedele F. 2007. Wave height distributions and nonlinear effects. *Ocean Engineering* 34(11-12):1631,1649 .

Yezzi A. & Soatto S. 2001 Stereoscopic Segmentation. *International Conference on Computer Vision*, 59-66

Zakharov VE. 1999. Statistical theory of gravity and capillary waves on the surface of a finite-depth fluid. *European Journal of Mechanics B-fluids* 18(3):327-34